Modeling the Role of Myosin 1c in Neuronal Growth Cone Turning

Feng-Song Wang, Can-Wen Liu, Thomas J. Diefenbach, and Daniel G. Jay
Department of Physiology, Tufts University School of Medicine, Boston, Massachusetts

ABSTRACT We addressed the mechanical basis for how embryonic chick dorsal root ganglion growth cones turn on a uniform substrate of laminin-1. Turning is significantly correlated with lamellipodial area but not with filopodial length. We assessed the lamellipodial contribution to turning by asymmetric micro-CALI of myosin isoforms that causes localized lamellipodial expansion (myosin 1c) or filopodial retraction (myosin V). Episodes of asymmetric micro-CALI of myosin 1c (or myosin 1c and V together) caused significant turning of the growth cone. In contrast, repeated micro-CALI of myosin V or irradiation without added antibody did not turn growth cones. These findings argue that lamellipodia and not filopodia are necessary for growth cone turning. To model the role of myosin 1c on growth cone turning, we fitted the measured trajectories from asymmetric micro-CALI of myosin 1c-treated and untreated growth cones to the persistent random walk model. The first parameter in this equation, root-mean-square speed, is indistinguishable between the two data sets whereas the second parameter, the persistence of motion, is significantly increased (2.5-fold) as a result of asymmetric inactivation of myosin 1c by micro-CALI. This analysis demonstrates that growth cone turning results from an increase in the persistence of directional motion rather than a change in speed. Taken together, our results suggest that myosin 1c is a molecular correlate for directional persistence underlying growth cone motility.

INTRODUCTION

Axon guidance is a key process in forming the precise pattern of the nervous system. It is governed by steering the motility of growth cones at the tips of growing axons (reviewed in Tessier-Lavigne and Goodman, 1996). The remarkable ability of growth cones to ''steer'' their way through the developing nervous system is enabled by several linked steps: actin-based protrusion of filopodia and lamellipodia at the growth cone periphery (see Fig. 1), engorgement by microtubules into the central domain of the growth cone, and consolidation of these microtubules to form the nascent axon (Mitchison and Kirschner, 1988). It was postulated that neurite outgrowth is controlled by the ''pull'' and ''push'' exerted by F-actin-mediated growth cone protrusion and anterograde movement of microtubules, respectively (Letourneau et al., 1987). We have focused on protrusion because drug-induced inhibition of actin polymerization collapses the leading edge and perturbs axon guidance both in vitro and in vivo (Marsh and Letourneau, 1984; Bentley and Toroian-Raymond, 1986). The molecular basis of protrusion remains unclear, but essential roles for the myosin superfamily of actin-based motors have been suggested (Lin and Forscher, 1995; Wang et al., 1996; Wylie et al. 1998). We had previously ascribed the roles of myosin isoforms in growth cones using microscale chromophore-assisted laser inactivation (micro-CALI) that inactivates a specific protein's function within a 10-μm region of the growth cones (Diamond et al., 1993). Inactivation of myosin V causes filopodial retraction whereas inactivation of myosin 1c (formerly Iβ) causes lamellipodial expansion (Wang et al. 1996; Diefenbach et al., 2002). Thus, using micro-CALI, we can independently and precisely alter filopodial and lamellipodial motility at the growth cone's leading edge. Recently, we have implicated myosin 1c as a motor involved in coupling retrograde flow to forward advance at the growth cone's leading edge (Diefenbach et al., 2002). In this article, we address the relative contributions of lamellipodia and filopodia to growth cone turning and the role that myosin 1c and V may play in turning events. With these results, we applied mathematical modeling to growth cone turning to further characterize the dynamics of growth cone turning and the potential contribution of myosin isoforms.

MATERIALS AND METHODS

Cell culture

Chick dorsal root ganglia from E10 to E12 embryos (Spafas, Norwich, CT) were dissociated with 0.25% trypsin in calcium/magnesium-free Hanks balanced salt solution (HBSS) and transferred to Leibovitz L-15 medium containing 10% FBS (Sigma Chemical, St. Louis, MO) and 25 ng/ml NGF (7S; Roche Applied Science, Indianapolis, IN). The neurons were then plated onto acid-cleaned glass coverslips (22 × 22 mm) coated with poly-L-lysine (1 mg/ml) followed by laminin (0.1 mg/ml in HBSS; Sigma Chemical) or laminin alone. The cultures were maintained at 37°C on the microscope stage with a stage incubator during the experiment. Selected neurons with growth cones possessing filopodial and lamellipodial morphology similar to the one shown in Fig. 1 were used for experiments.

Microscopy

A phase-contrast inverted microscope (Zeiss Axiovert 10, Carl Zeiss Microimaging, Thornwood, NY) was used to monitor growth cone movements. Time-lapse images were taken at one frame every 15 s, digitally enhanced by custom-written software and recorded on an optical memory disk recorder (Panasonic, Secaucus, NJ). Growth cone and neurite

Submitted February 6, 2003, and accepted for publication June 4, 2003.

Address reprint requests to Daniel G. Jay, E-mail: daniel.jay@tufts.edu.
Feng-Song Wang's present address is Dept. of Biological Sciences, Purdue University, Calumet, 2200 169th St., Hammond, IN 46323.

0006-3495/03/11/3319/10 $2.00

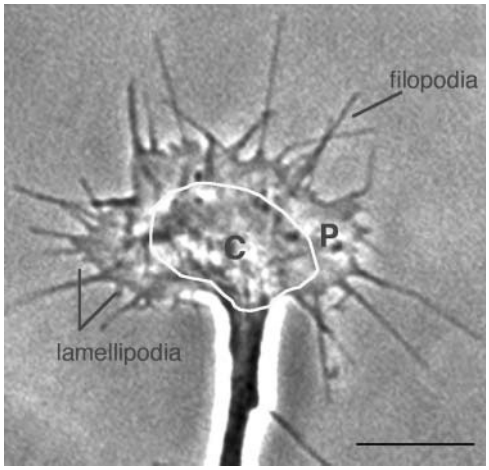

FIGURE 1 A chick dorsal root ganglion neuronal growth cone is shown delineating the central (*C*) and peripheral (*P*) domains. In the peripheral domain, fingerlike projection called filopodia and veils between them called lamellipodia are indicated. Scale bar = 10 μm.

parameters such as filopodial length, lamellipodial size, neurite neck position, and growth cone turning angles were measured and analyzed using NIH image software (National Institutes of Health, Bethesda, MD) on a Macintosh-based desktop computer.

The length and number of filopodia as well as the lamellipodial area were measured from the recorded images at 1-min intervals. The rate and trajectory of neurite extension were traced and measured from the center of neurite neck. The neurite extension direction was determined by the direction of the last 5-μm segment of the neurite at the neck of growth cones according to Song et al. (1997). The turning angle was deduced from the differences between the direction of neurite extension at the onset and at the end of the experiment period.

Detachment experiment

Cell bodies and neurite shafts were physically detached from the substrate with a microjet of warm medium from a micropipette generated by a custom-made pressure control unit (Yu-Li Wang, University of Massachusetts Medical School, Worcester, MA) as described in Gundersen and Barrett (1980). The rate of growth cone translocation was calculated based on the changes in *x*-*y* position of the neurite neck positions.

Asymmetric micro-CALI of myosin 1c and V

MG-labeled antibodies (affinity purified anti-myosin V polyclonal antibody (Espreafico et al., 1992) and anti-myosin 1c monoclonal antibody (M2) (Wagner et al., 1992) at 1 mg/ml were mixed with fluorescein-dextran at 1-mg/ml final concentration (Molecular Probes, Eugene, OR) and micro-injected into the cell bodies of selected neurons. After 30–60 min, healthy neurons were chosen for asymmetric micro-CALI experiments. Each growth cone was observed for 5 min, then one-half of the growth cone area was subjected to laser irradiation for 5 min and observed for 5 min. This procedure was repeated 5× during a 1-h experiment period. The microscope stage was adjusted to ensure that the same part of a growth cone was laser-irradiated during each experiment. The laser beam for micro-CALI was generated using a nitrogen-pumped pulsed dye laser (model VSL-337, Spectra Physics, Mountain View, CA) at an energy output of 30-μJ/pulse (10-μm diameter laser spot) with a pulse width of 1 ns and a 20-Hz frequency. Healthy growth cones that extended >20 μm during a 1-h observation period were used for the statistical analysis using StatView II software (Cherwell Scientific Publishing, Palo Alto, CA).

Growth cone motion parameters

To model growth cone motility, movement of individual growth cones was quantified by measurements of the positions of growth cone centroids at regular time intervals. The time interval between subsequent measurements was chosen to be 1 min, which we took as a suitable time frame for observing growth cone dynamics. We also measured the positions of neurite neck points at each timepoint. The measurements are illustrated in Fig. 1, which shows a typical DRG growth cone and the attached neurite shaft. The outline of the growth cone was obtained by manually tracing the lamellipodial periphery, leaving out filopodia (defined here to have diameters of <0.5 μm). The position of growth cone centroid was then calculated as the mean values of the coordinates of all the points on and within the outline, i.e., center of area. The mean values of all the points on the outline alone gives the center of outline (or, the center of boundary), which can alternatively be used as a measure of the growth cone position (Soll and Voss, 1998). Here, we used center of area as growth cone centroids. Sequential connections of such discrete centroid positions provide an estimate of the true growth cone trajectory. Sequential connections of neurite neck points constitute the neurite trajectory. To account for stage movements during time-lapse recording, a fixed particle on the coverslip was also measured at each frame to serve as a reference point. The estimated error in the determination of centroid position is <0.2 μm, based on the reproducibility of an outline in 10 repeat measurements of a single growth cone and the error in the measurement of the reference particle.

The persistent random walk model

We applied the concept of persistent random walk to model growth cone motility (Uhlenbeck and Ornstein, 1930). This model has been used to describe the random movement of other cell types (Alt, 1990; Dunn, 1983; Gail and Boone, 1970; Othmer et al., 1988). A persistent random walk differs from a pure random walk (Berg, 1993) in that correlation between successive movement steps is taken into account. For a two-dimensional cell movement, Gail and Boone (1970) derived the mean-squared displacement from a series of discrete displacement segments when the effects of persistence were considered as

$$\langle d2\rangle = 2\alpha/\beta 3(\beta t - 1 + e - \beta t), \qquad (1)$$

where α and β are related to two physical parameters, characteristic speed S, and persistence of velocity P_v where $S = (\alpha/\beta)1/2$ and $P_v = 1/\beta$. With the definition of the root-mean-square speed S and the directional persistence time P_v, Dunn (1983) obtained: 1), the first term on the right-hand side of Eq. 1 is linear with the time interval t, similar to that of the pure random walk; 2), the second term in the parentheses is the correction due to the correlation between successive movement steps; and 3), the strength of such a correlation is characterized by the parameter P_v, the directional persistence time. Eq. 1 was also obtained by Othmer et al. (1988) based on a Poisson process for velocity changes, and by Alt (1990) based on correlation analysis of two-dimensional velocity vectors. Conceptually, S is an averaged measure of the magnitude of the instantaneous velocity, and P_v is an averaged measure of the time duration before which a significant change in the direction of movement occurs.

Application of the persistent random walk model to growth cone movement

For each growth cone, the mean-squared displacement at time interval t was calculated by summing over the squared distances from all displacements that span time t and then divided by the number of such time intervals. We used overlapping time intervals (e.g., 0–2 min, 1–3 min, 2–4 min, etc., for the time interval t = 2 min) to make full use of all measurements available (DiMilla et al., 1993; Stokes and Lauffenburger, 1991). At larger time intervals, there are fewer datapoints available for the calculation of mean-

squared displacements and this fact renders these values statistically less reliable. For this reason, we also calculated the expected variance in the mean-squared displacements. The data were then fit to Eq. 1 by a nonlinear least-square procedure (Press et al., 1986), weighted inversely to the expected variance, to obtain the best values of the model parameters speed S and persistence time P_v. We also treated the growth cones as a population and calculated the pooled mean-squared displacements from all the growth cone trajectories. The pooled data was then fitted to the model by the same procedure. These analyses are similarly applied to the movement of neurite neck points. As one growth cone in our study was only tracked for 45 min, we only used trajectories between 0 and 45 min to calculate the pooled values. For individual growth cones, we used full-length trajectories to calculate, but only those for time intervals of 45 min were used to fit Eq. 1.

Coordinate transformation and statistical analysis

To compare the trajectories of growth cones treated with asymmetric micro-CALI of myosin 1c and untreated growth cones, the coordinates of growth cone centroids were transformed into a new coordinate system, where the growth cone centroid at time zero is at the new origin and the neurite direction at time zero is positioned along the ^{+}y-axis. For the three (out of eight) growth cones treated with asymmetric micro-CALI of myosin 1c on the left sides of the growth cones, they were flipped so that the irradiation sides are in the first quadrant. For the untreated growth cones, the same proportion (3/8 $\sim$ 37.5%) of growth cones was randomly chosen to flip sides. This is because DRG neurites have the tendency to grow clockwise (data not shown; P. C. Letourneau, personal communication), similar to the growth of retinal explants (Heacock and Agranoff, 1977). Statistical comparisons of the motility parameters for growth cones treated with asymmetric micro-CALI of myosin 1c and untreated ones were done by Student's unpaired t-test with unequal variances (Devore, 1991). For the pooled values of the mean-squared displacements for each of the two groups of growth cones, the uncertainties for the best-fit parameters were determined using the upper 5% of the F-distribution (Beale, 1960; Pearson and Harley, 1970).

RESULTS

Growth cone motility and turning are thought to occur through the processes of leading edge protrusion and microtubule-based engorgement. To isolate the specific contribution of leading edge protrusion, we physically detached the somata and neurites from their laminin-1 substrate with microjets of cell culture medium (Gundersen and Barrett, 1980). Growth cones with detached somata move 5$\times$ faster than growth cones with attached somata (Fig. 2 *A*). Furthermore these growth cones showed significantly more frequent turning when unhindered by the soma and neurite shaft (Fig. 2 *B*), possibly because engorgement by microtubules from the neurite may stabilize growth cone direction. The average net deviation from the initial outgrowth direction was 26.3° $\pm$ 4.6 ($n = 12$) for the detached neurons compared to 2.2° $\pm$ 0.5 ($n = 9$) for attached neurons over the 20-min sampling interval ($p < 0.001$; Fig. 2 *B*). The increased turning of these unconstrained growth cones allowed us to correlate growth cone turning with the behavior of filopodia and lamellipodia at the leading edge. Of the 12 growth cones examined, eight exhibited turning (as defined by a turning angle >10° during a 20-min observation period). We compared each half of these eight growth cones and assessed

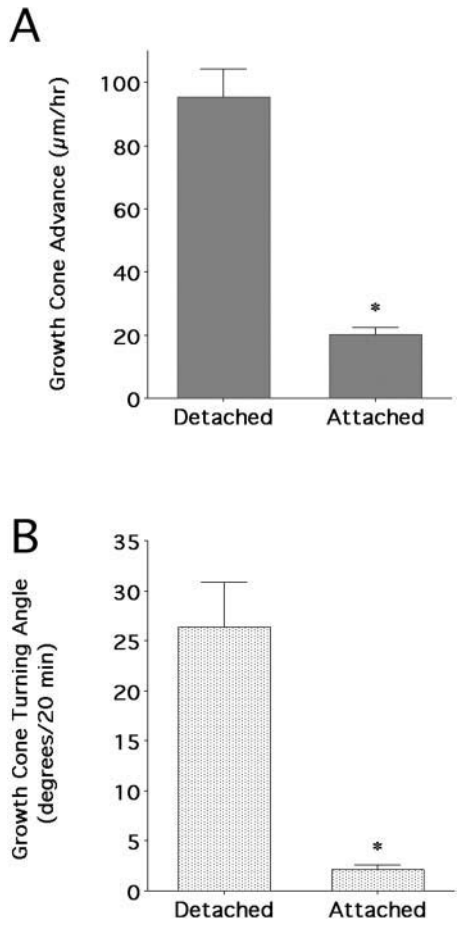

FIGURE 2 Fast advance of the neuronal growth cone under the condition of soma and neurite shaft detachment observed during a 20-min experiment period. (*A*) The rate of neuronal growth cone advance under the condition of soma and neurite shaft detachment was ~5$\times$ faster than that of the normal neurite extension. (*B*) Growth cone turned more frequently without being hindered by the soma and neurite shaft. The error bars represent mean $\pm$ SE and the asterisks indicate significant differences between detached and attached growth cones ($p < 0.01$ by Student's t-test).

lamellipodial area, filopodial number, and length during turning. Lamellipodia on the side toward which the growth cone turned were significantly larger than those on the opposite side (58.4% $\pm$ 2.0 vs. 41.6% $\pm$ 2.0; $p < 0.01$; Fig. 3 *A*). In contrast, there were no significant differences between average filopodial lengths (10.1 μm $\pm$ 0.6; 9.7 μm $\pm$ 0.5; $p > 0.5$; Fig. 3 *B*), or average filopodial numbers (5.1 $\pm$ 0.4; 5.8 $\pm$ 0.4; $p > 0.1$; Fig. 3 *C*) on the two sides. No significant asymmetric distribution of lamellipodia was observed for growth cones exhibiting turning angles <10° during the 20-min observation period (data not shown). These findings correlate the asymmetric distribution of growth cone lamellipodia with the direction of growth cone turning and suggest that growth cone turning is mediated by lamellipodia rather than filopodia.

To directly test this hypothesis, we used micro-CALI to inactivate myosin 1c and myosin V asymmetrically across

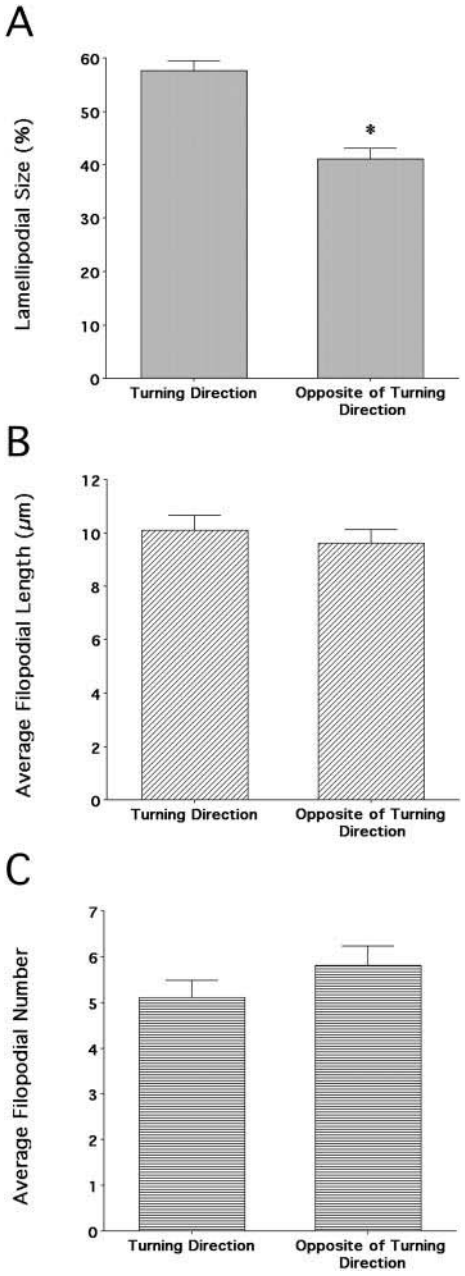

FIGURE 3 Lamellipodial asymmetry is correlated with growth cone turning of neurons with detached somata and neurites. The data show the percentage of lamellipodial size as well as the average number and length of filopodia on two sides of the growth cone as defined by a line drawn along the direction of neurite extension. (*A*) Lamellipodial size on the side of the turning direction of the growth cone is significantly larger than that on the side opposite of the turning direction. (*B*) Average filopodial length showed no difference. (*C*) Average filopodial numbers were not significantly different. The error bars represent mean ± SE and the asterisk indicates significant difference (* $p < 0.01$) by Student's paired *t*-test. Comparisons between other groups were not statistically different ($p > 0.05$).

DRG growth cones. Previously, we showed that these two myosin isoforms play differential roles in lamellipodial and filopodial motility (Wang et al., 1996; Diefenbach et al., 2002). Asymmetric micro-CALI of myosin 1c in growth cones induced a significant lamellipodial protrusion without affecting filopodial motility (Wang et al., 1996; Diefenbach et al., 2002). In contrast, asymmetric micro-CALI of myosin V causes a net filopodial retraction over time without affecting lamellipodia. If lamellipodial protrusion is required for turning, then induced lamellipodial expansion by asymmetric micro-CALI of myosin 1c on one side of the growth cone should steer subsequent movement toward that side. If filopodial protrusion is necessary for turning, then induced filopodial retraction by asymmetric micro-CALI of myosin V on one side should turn growth cones away from that side.

Although untreated growth cones moved in random directions, they grew straight on average and had an average turning angle near zero ($-2.3° \pm 2.6°$, $n = 9$). A single 5-min period of asymmetric micro-CALI of myosin 1c caused lamellipodial expansion without obvious growth cone turning (Wang et al., 1996), likely because turning requires prolonged lamellipodial asymmetry (Chang et al., 1995). However, when one side of a DRG growth cone was subjected to five, 5-min periods of micro-CALI of myosin 1c within a 1-h period, growth cone turning occurred toward the side of irradiation (Fig. 4). Within 60 min, the asymmetric application of micro-CALI of myosin 1c caused a significant deviation of growth cones from the initial axis of outgrowth (Fig. 4 *A*). Similar results were obtained when asymmetric micro-CALI of myosin 1c and V were performed simultaneously (Fig. 4 *B*). In contrast, asymmetric micro-CALI of myosin V alone (Fig. 4 *C*) or asymmetric micro-CALI of growth cones loaded with MG-labeled nonimmune IgG (Fig. 4 *F*) did not cause a significant deviation of growth cones from the initial axis of outgrowth. The trajectories of neurite extension for all treatments are illustrated in composite drawings shown in Fig. 4, *D–G*. Fig. 4 *D* shows that neurites turn toward the side of laser irradiation when myosin 1c was asymmetrically inactivated. The average turning angle after asymmetric micro-CALI of myosin 1c was significantly different from the angle observed with control (untreated) neurons ($9.6° \pm 4.4$, $n = 10$ vs. $-2.3° \pm 2.6$, $n = 9$; $p < 0.05$; Fig. 5 *A*). These findings show that repeated expansion of lamellipodia on one side of a growth cone can turn the growth cone toward this side and that loss of myosin 1c contributes to this process.

The contribution of filopodia in growth cone turning was examined by subjecting growth cones to asymmetric micro-CALI of myosin 1c and myosin V (Fig. 4 *B*) in combination or myosin V alone (Fig. 4 *C*). Repeated asymmetric micro-CALI of myosin V did not affect the direction of growth cone advance ($-0.2° \pm 0.3°$, $n = 8$; Fig. 4 *C*). Net growth cone turning was not observed, although these growth cones showed more robust wandering. Furthermore, asymmetric micro-CALI of myosin 1c and V together induced significant growth cone turning toward the laser-irradiated side that was similar to the turning caused by asymmetric micro-CALI of myosin 1c alone ($11.5° \pm 4.3$, $n = 7$ vs. $-2.3° \pm 2.6$, $n = 9$; $p < 0.01$; see also Fig. 4 *C*). A comparison of these

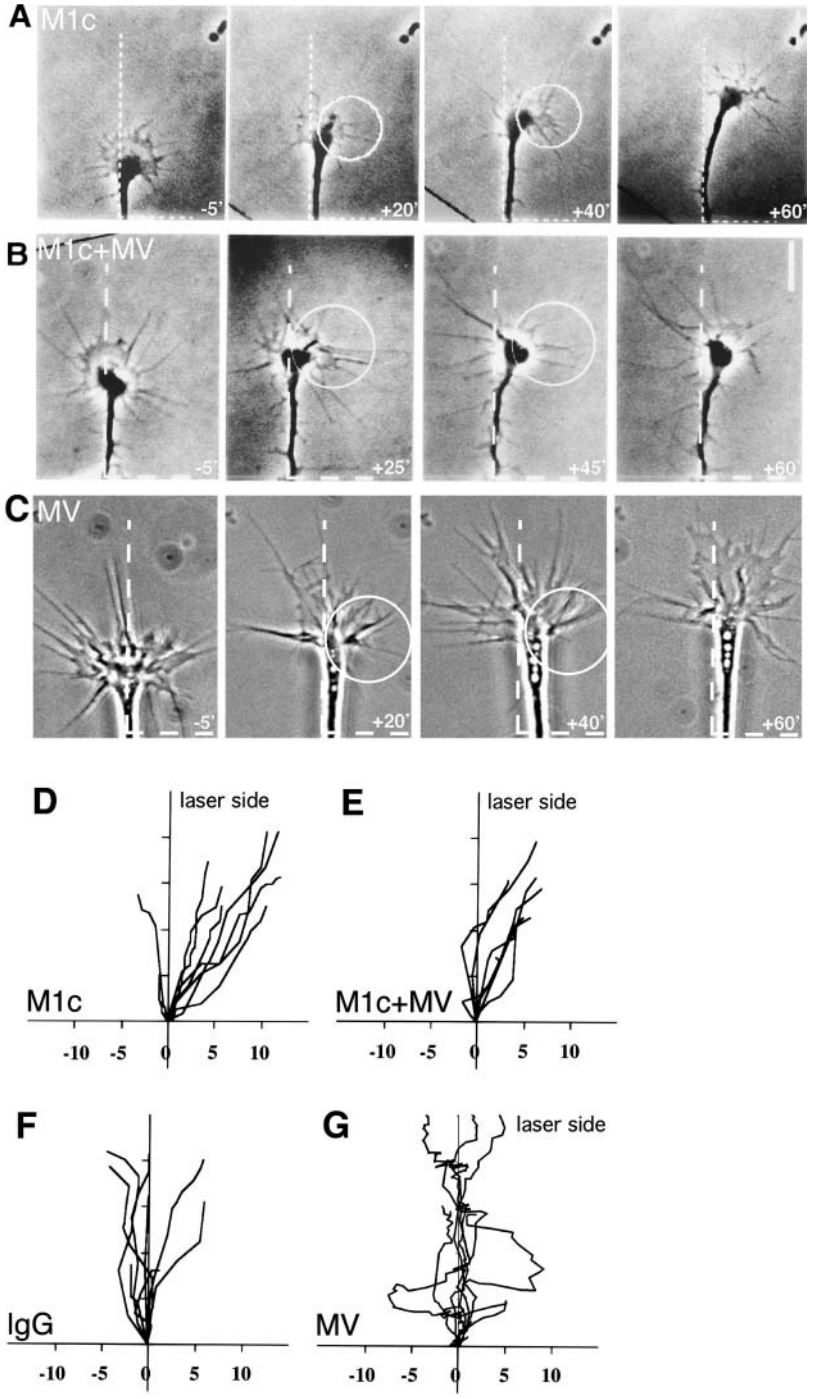

FIGURE 4 Comparison of turning achieved by asymmetric micro-CALI of myosin 1c alone, myosin V alone, or both myosin 1c and myosin V simultaneously. (*A–C*) Series of phase images showing that selected growth cones of neurons injected with MG-myosin 1c antibody (*A*), or MG-anti-myosin 1c and MG-anti-myosin V antibodies together (*B*), or MG-anti-myosin V antibody alone (*C*), that were laser-irradiated repeatedly on half of the growth cones. The numbers are the time in minutes after the initiation of the first period of laser irradiation. The circles indicate the area of laser irradiation. Note that the growth cones turned toward the side of laser irradiation in *A* and *B*, but not in *C*. Scale bar, 10 μm. (*D–G*) Composite drawings of neurite neck positions for neurons injected with MG-anti-myosin 1c (*D*), MG-anti-myosin 1c and MG-anti-myosin V (*E*), MG-IgG (*F*), or MG-anti-myosin V (*G*) examined over the 1-h experimental period. The origin represents the initial position of the center of the growth cone neck at 5 min before the initiation of laser irradiation. The original direction of neurite extension, as defined by the direction of the last 5-μm segment of the neurite at the onset of experiments, was aligned with the vertical line. The original orientation of the growth cone was positioned such that the laser-irradiated half of the growth cone was on the right side of the graph. Tick marks on both axes, 5 μm.

treatments is presented in Fig. 5 *A*. Asymmetric micro-CALI of myosin 1c resulted in significant deviations from straight-line extension (9.6° ± 4.4, $n = 10$). Double inactivation of myosin 1c and myosin V together resulted in turning that was similar to that caused by inactivation of myosin 1c alone (11.5° ± 4.3, $n = 7$ vs. 9.6° ± 4.4, $n = 10$; $p > 0.10$). In contrast, asymmetric micro-CALI of myosin V alone did not cause significant turning. None of these treatments altered the rate of neurite extension (Fig. 5 *B*). Thus, repeated and prolonged asymmetric filopodial retraction does not alter growth cone direction. Together, our findings support the hypothesis that lamellipodial and not filopodial motility is the major mechanical determinant of DRG growth cone turning. They also illustrate that turning is evoked by asymmetric loss of myosin 1c, and this suggests that guidance cues that can locally modulate myosin 1c may also evoke turning.

To further analyze the role of myosin 1c in growth cone turning, we quantitated the trajectories of the growth cone centroid during the asymmetric micro-CALI of myosin 1c

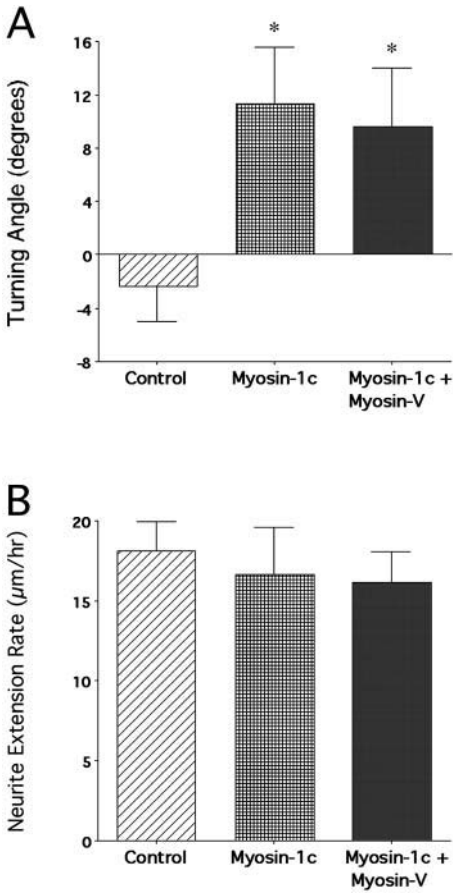

FIGURE 5 Turning responses of growth cones, following the asymmetric inactivation of myosin 1c or myosin 1c and myosin V observed during 1-h experiment period. (*A*) The average turning angle of the growth cones of the examined neurons. (*B*) The average rate of neurite extension of the examined neurons. The error bars represent mean ± SE and the asterisks indicate significant difference between control and experimental groups ($p < 0.05$) by Student's unpaired *t*-test. Comparisons between other groups were not statistically different ($p > 0.05$).

and modeled these data. This quantitative analysis and modeling provides a concise and objective description of growth cone motility and enables the detection of subtle differences in motility caused by treatments that may not be obvious through qualitative observation (Dunn and Brown, 1987). First, mean-squared displacements of centroids from untreated growth cones were calculated at each time-lapse image. We then fitted these data to a mathematical model based on the Langevin equation that describes growth cone movement as a persistent random walk (Eq. 1), where the growth cone motility is characterized by two parameters: the speed S and the directional persistence time P_v.

Fig. 6, *A–C*, shows plots of mean-squared displacement versus time (*solid symbols*) for three typical untreated growth cones calculated for time intervals up to 45 min. The solid curves represent weighted fits to the persistent random walk model (Eq. 1). We see that individual growth cone movement can be described well by the model for the time range examined. For time intervals $>\sim$45 min, the fitting is less satisfactory, probably due to insufficient data available for the calculation of the parameters (Stokes and Lauffenburger, 1991; DiMilla et al., 1993). The average speed and persistence time for all 10 growth cones examined is $S = 0.42 \pm 0.04$ μm/min and $P_v = 38.3 \pm 9.5$ min. These values are similar to the corresponding values for the neurite neck points ($S = 0.45 \pm 0.05$ μm/min; $P_v = 39.1 \pm 8.6$ min).

We also modeled the mean-square displacement as a function of time for trajectories of growth cones subjected to asymmetric micro-CALI of myosin 1c. These data sets also showed good agreement between the model and the mean-squared displacements calculated up to 45 min. Compared to untreated neurons, asymmetric micro-CALI of myosin 1c-treated growth cones advanced at similar speeds but with significantly higher persistence times ($S = 0.42 \pm 0.05$ μm/min and $P_v = 85.2 \pm 23.7$ min, $n = 8$, mean ± SE, vs. $S = 0.42 \pm 0.04$ μm/min and $P_v = 38.3 \pm 9.5$ min for untreated neurons, $p < 0.05$). In Fig. 7, *A* and *B*, we show growth cone trajectories (between 0 and 45 min) for each group in the new coordinate system (see Materials and Methods). We observed that the untreated growth cones showed tortuous trajectories that were symmetric about the *y*-axis. In contrast, growth cones treated with asymmetric micro-CALI of myosin 1c had smoother paths and were skewed toward the ^{+}x-axis. Fig. 7, *C* and *D*, shows the pooled values of the mean-squared displacements for each group of growth cones (*solid curves*) calculated from all the trajectories shown in Fig. 7, *A* and *B*, respectively. There is good agreement between the displacement data (*solid lines*) and the persistent random walk model (*dotted lines*) for both untreated and CALI-treated growth cones. The speeds were indistinguishable for the two data sets: $S = 0.43 \pm 0.01$ μm/min for untreated growth cones compared to $S = 0.43 \pm 0.01$ μm/min for CALI-treated growth cones. However, persistence times were significantly different ($p < 0.05$). Growth cones treated with asymmetric micro-CALI of myosin 1c had $\sim$2.5-fold longer persistence times ($P_v = 82.7 \pm 25.0$ min compared to $P_v = 33.2 \pm 3.6$ min for untreated growth cones). This greater persistence time for the micro-CALI-treated growth cones is consistent with their relatively smoother paths (Fig. 7 *B*) as compared to the more tortuous paths of untreated growth cones (Fig. 7 *A*).

DISCUSSION

Our focus has been to understand directed growth cone motility (Jay, 2000). Here we report a statistical correlation between lamellipodial expansion (but not filopodial motility) and the subsequent direction of growth cone turning. These findings suggest that the asymmetry of lamellipodia alone can turn growth cones and suggest that filopodial motility do not contribute to the mechanical aspects of growth cone turning. We supported these hypotheses by the following experiments. When lamellipodia were asymmetrically

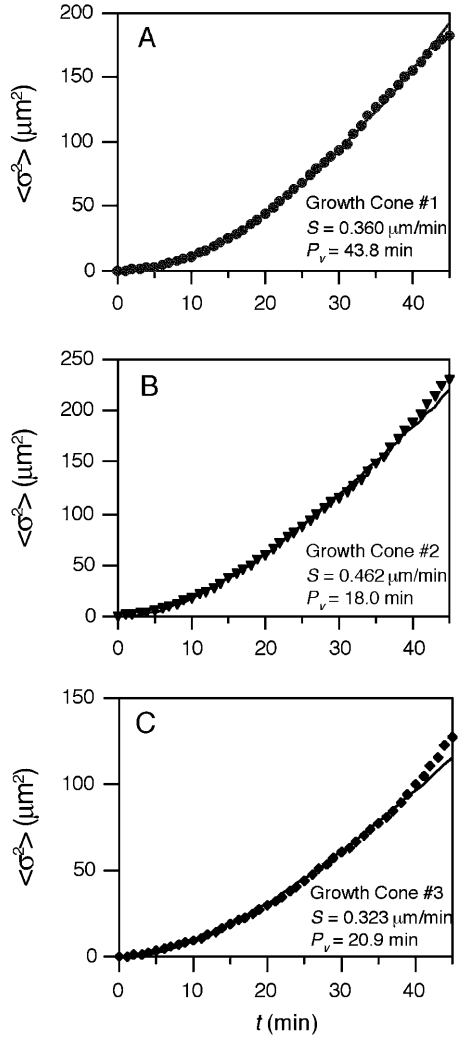

FIGURE 6 Fitting single untreated growth cone trajectories to the persistent random walk model (Eq. 1). The calculated mean-squared displacements were shown as solid symbols and the weighted fits to the persistent random walk model were shown in solid lines. The best fitting parameters for S, the speed, and P_v, the persistence time, were shown for each growth cone.

expanded by micro-CALI of myosin 1c, growth cones turned toward this area of expansion. In contrast, localized filopodial retraction by asymmetric micro-CALI of myosin V had no effect on growth cone turning. Finally, when growth cone motility on a uniform, permissive substrate is analyzed, the displacement can be well modeled by a biased random walk equation showing that growth cones subjected to asymmetric loss of myosin 1c undergo a marked change in directional persistence without a significant change in speed. Our findings suggest that lamellipodial protrusion is the mechanical basis of growth cone turning. Lamellipodia have greater adhesive contact with the underlying substrate than filopodia (Zheng et al., 1994a,b) and are thus more likely to participate in local growth cone protrusion.

It has been postulated that filopodia initiate turning of growth cones (O'Connor et al., 1990; Kuhn et al., 1998; Gomez et al., 2001). However, grasshopper pioneer neurons in vivo show no correlation between filopodial number and growth cone direction (Isbister and O'Connor, 1999). Filopodia indeed act in growth cone turning but they likely do so by acting as sensory antennae (Davenport et al., 1993) that sample environmental cues, relay these signals to the rest of the growth cone (Zheng et al., 1996; Song et al., 1997), and initiate adhesive contacts (Kuhn et al., 1995). When growth cones encounter guidance cues or asymmetric environments, signaling changes may also affect filopodial motility and distribution (Zheng et al., 1996) or microtubule engorgement (Burmeister et al., 1991) to guide subsequent growth cone motility. Interestingly when filopodia are disrupted by inhibition of actin polymerization, growth cones move forward but tend to wander (Marsh and Letourneau, 1984). After asymmetric micro-CALI of myosin V we also observed that growth cones would wander (though did not exhibit net turning after 1 h) consistent with these previous studies.

We have shown that induced asymmetric activity of myosin 1c can turn growth cones. Support for a role of class I myosins in directing cell migration also comes from genetic studies in *Dictyostelium*. Deletion of myosin-1 induced a more frequent turning of cells (Wessels et al., 1996) whereas overexpression hindered the ability of cells to migrate, perhaps due to an increase in tension between cortical cytoskeleton and membrane (Novak and Titus, 1997). The molecular mechanism underlying myosin 1c function in lamellipodia is unclear. The binding of myosin 1c to phospholipids, its localization at the periphery, and its slow kinetics are most consistent with a role of myosin 1c in binding cortical F-actin to the plasma membrane (Collucio, 1997; Jay, 2000). As such it has the potential to act as a molecular clutch during leading edge protrusion as envisioned by Mitchison and Kirschner (1988). We have no data to suggest how myosin 1c may act as a molecular clutch except that its localized loss decreases retrograde flow as assessed by fiduciary beads (Diefenbach et al., 2002). Myosin 1c can bind to lipids and membranes and is thought to be able to move actin filaments as a cohort and is regulated by calcium via calmodulin that serves as its activating light chain (reviewed in Collucio, 1997). Growth cones turn in response to localized changes in intracellular calcium evoked by environmental cues (Zheng et al., 1994a,b; Takei et al., 1998). Based on these studies, we speculate that environmental cues may turn growth cones through generating local changes in growth cone morphology perhaps by calcium-mediated regulation of myosin 1c. In general, growth cone turning may require the asymmetric modulation of proteins, such as myosin 1c, that are involved in mechanical aspects of growth cone motility.

Here, we have modeled growth cone motility using the persistent random walk model and found that asymmetric functional loss of myosin 1c affected growth cone persistence time but not speed, with the effect of increasing

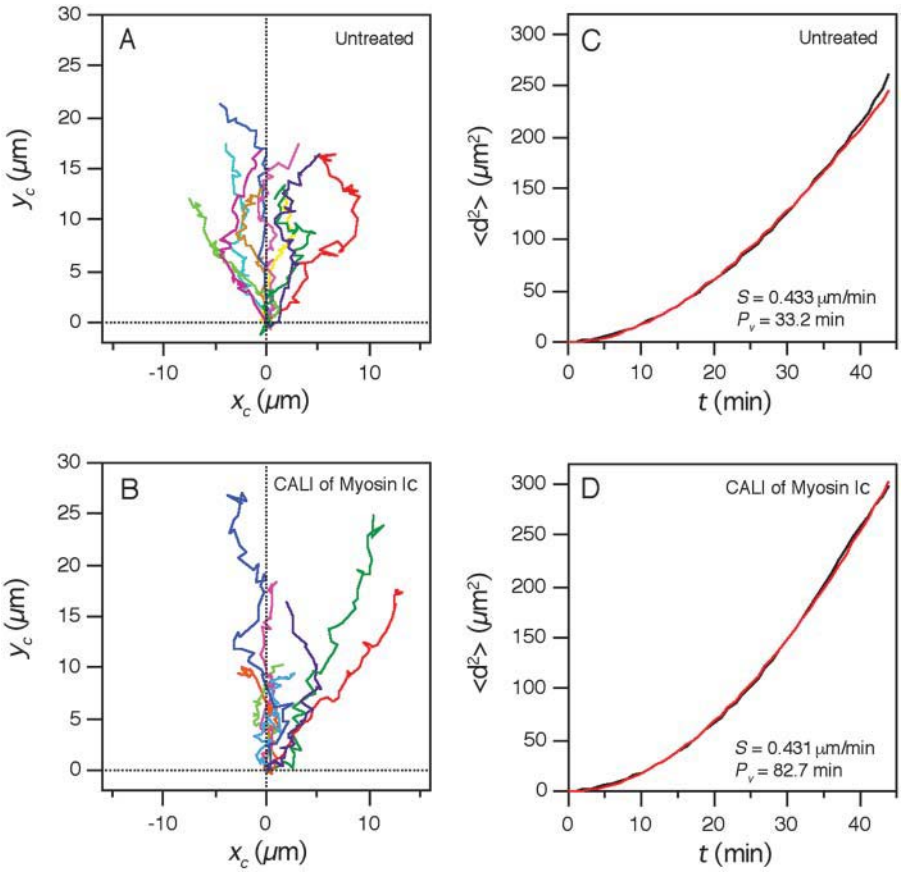

FIGURE 7 Fitting pooled data sets to the persistent random walk model (Eq. 1) for untreated and CALI-treated growth cones. The growth cone trajectories (*A*, *B*) and the pooled values of the mean-squared displacements (*C*, *D*; *lines in black*) for the untreated growth cones and the growth cones treated with asymmetric micro-CALI of myosin 1c, respectively. The trajectories are plotted in the new coordinate system (see Materials and Methods) for the time duration between 0 and 45 min. The mean speed and persistence time, obtained from weighted nonlinear least square fit (*lines in red*) of the persistent random walk model, were shown in each plot, respectively.

both the path length and the dispersion of the growth cones proportionally. This is surprising because it was thought unlikely that a treatment would affect the persistence alone (Dunn and Brown, 1987). Our explanation for this is that our treatment is not an external agent but a direct and asymmetric change in the activity of an actin-based motor protein, myosin 1c, within the growth cones. The asymmetric distribution of this motor protein might have affected the cytoskeletal elements that control the direction but not the speed of growth cone movement. Fine scale analysis of the motion suggests that growth cones change their direction at high frequency, perhaps as part of the searching process that must occur during axon guidance. The perturbation of myosin 1c affects this oscillatory motion such that movement is persistent in one direction (i.e., toward the laser spot). The analysis presented here suggests a balance of forces in actin-based motility that is disrupted when one myosin isoform is lost asymmetrically across the growth cone. Under normal conditions there is a dynamic balance of tension such that the two sides alternatively win the tug of war across the growth cone and directional persistence times are short. Growth cones show an oscillatory ''wig-wag'' movement perhaps to better explore its environment for guidance cues. When myosin 1c was asymmetrically inactivated, the growth cone ''wigs'' more than ''wags'' such that the growth cone turns toward the irradiated side.

It is not known how myosin 1c activity controls growth cone movement. Understanding the cellular processes affected by myosin 1c loss may lead to insights into these molecular mechanisms. One study sheds light on how myosin 1c might affect a proposed balance of forces across the growth cone (Diefenbach et al., 2002). Micro-CALI of myosin 1c causes a loss of retrograde flow and a concomitant protrusion of the lamellipodial leading edge, likely due to increased actin polymerization during reduced retrograde flow (Diefenbach et al., 2002). In the current experiments, repeated asymmetric loss of myosin 1c causes turning toward the irradiated side and this is associated with an increased persistence of direction. Myosin 1c may act to pull back the leading edge by its action in retrograde flow. When myosin 1c is disrupted asymmetrically and repeatedly, there is a loss of retrograde flow such that there is net lamellipodial protrusion on the irradiated side. This summing of forces resolve in favor of one side of the growth cone and thus directional persistence is increased.

Although myosin 1c acts to pull the actin cytoskeleton back by retrograde flow, other myosins could generate the tension necessary to pull the leading edge of the growth cone forward. Myosin II is a likely candidate for this, based on its relative abundance in growth cones (Wylie et al., 1998). Indeed, when myosin II function was disrupted by micro-CALI, lamellipodial retraction occurred, suggesting a role

for this isoform in leading edge protrusion (Diefenbach et al., 2002). Paradoxically, myosin II may also act in growth cone collapse as it is implicated downstream of collapsing factors. This may occur when leading edge adhesion is weak and myosin II has a general role of exerting tension between actin filaments in lamellipodia. This is analogous to its role in contracting muscle where myosin acts to draw actin filaments closer together. Thus, when actin at the leading edge is well-anchored, growth cones pull themselves forward; and when the leading edge is not anchored, growth cones pull back (i.e., retract).

In closing, we suggest that mathematical modeling can contribute to the rudiments of a physical (albeit statistical) understanding of growth cone motility. Using localized molecular perturbation provided by micro-CALI, we were able to attribute local in situ function of a specific protein to a specific cellular process. The coupling of mathematical and biochemical approaches may allow for a greater understanding of how the protein-based machinery in cells generates motility. We believe that the coupling of theory-based and experimental methods will have increasing importance in addressing complex cellular processes.

We thank R. E. Cheney, M. S. Mooseker, and J. P. Albanesi for providing antibodies.

This work was supported in part by grants to D.G.J. from the National Institutes of Health (NS34599 and EY11992). F.S.W. acknowledges receipt of an NSRA postdoctoral fellowship from the National Institutes of Health. C.W.L. was supported by a postdoctoral fellowship from the Program in Mathematics and Molecular Biology, with funding from the National Science Foundation under grant DMS-9406348.

REFERENCES

Alt, W. 1990. Correlation analysis of two-dimensional locomotion paths. *In* Lecture Notes in Biomathematics: Biological Motion Process. W. Alt, and G. Hoffmans, editors. Springer-Verlag, New York. 254–268.

Beale, E. M. L. 1960. Confidence regions in non-linear estimation. *J. Royal Stat. Soc. B.* 22:41–76.

Bentley, D., and A. Toroian-Raymond. 1986. Disoriented pathfinding by pioneer neurone growth cones deprived of filopodia by cytochalasin treatment. *Nature.* 323:712–715.

Berg, H. C. 1993. Random Walks in Biology, 2nd Ed. Princeton University Press, Princeton.

Burmeister, D. W., R. J. Rivas, and D. J. Goldberg. 1991. Substrate-bound factors stimulate engorgement of growth cone lamellipodia during neurite elongation. *Cell Motil. Cytoskeleton.* 19:255–268.

Chang, H. Y., K. Takei, A. M. Sydor, T. Born, F. Rusnak, and D. G. Jay. 1995. Asymmetric retraction of growth cone filopodia following focal inactivation of calcineurin. *Nature.* 376:686–690.

Coluccio, L. M. 1997. Myosin I. *Am. J. Physiol.*273:C347–C359.

Davenport, R. W., P. Dou, V. Rehder, and S. B. Kater. 1993. A sensory role for neuronal growth cone filopodia. *Nature.* 361:721–724.

Devore, J. L. 1991. Probability and Statistics for Engineering and the Sciences. Wadsworth, Belmont, CA.

Diamond, P., A. Mallavarapu, J. Schnipper, J. W. Booth, L. Park, T. P. O'Connor, and D. G. Jay. 1993. Fasciclin I and II have distinct roles in the development of grasshopper pioneer neurons. *Neuron.* 11:409–421.

Diefenbach, T. J., V. Latham, D. Yimlamai, C. W. Liu, I. M. Herman, and D. G. Jay. 2002. Myosin 1c and IIB serve opposing roles in lamellipodial movements in the neuronal growth cone. *J. Cell. Biol.* 158:1207–1217.

DiMilla, P. A., J. A. Stone, J. A. Quinn, S. M. Albelda, and D. A. Lauffenburger. 1993. Maximal migration of human smooth muscle cells on fibronectin and type IV collagen occurs at an intermediate attachment strength. *J. Cell Biol.* 122:729–737.

Dunn, G. A. 1983. Characterizing a kinesis response: time-averaged measures of cell speed and directional persistence. *Agents Actions Suppl.* 12:14–33.

Dunn, G. A., and A. F. Brown. 1987. A unified approach to analysing cell motility. *J. Cell Sci. Suppl.* 8:81–102.

Espreafico, E. M., R. E. Cheney, M. Matteoli, A. A. Nascimento, P. V. De Camilli, R. E. Larson, and M. S. Mooseker. 1992. Primary structure and cellular localization of chicken brain myosin V (p190), an unconventional myosin with calmodulin light chains. *J. Cell Biol.* 119:1541–1557.

Gail, M. H., and C. W. Boone. 1970. The locomotion of mouse fibroblasts in tissue culture. *Biophys. J.* 10:980–992.

Gundersen, R. W., and J. N. Barrett. 1980. Characterization of the turning response of dorsal root neurites toward nerve growth factor. *J. Cell Biol.* 87:546–554.

Heacock, A. M., and B. W. Agranoff. 1977. Clockwise growth of neurites from retinal explants. *Science.* 198:64–66.

Isbister, C. M., and T. P. O'Connor. 1999. Filopodial adhesion does not predict growth cone steering events in vivo. *J. Neurosci.* 19:2589–2600.

Jay, D. G. 2000. The clutch hypothesis revisited: ascribing the rolls of actin-associated proteins in filopodial protrusion in the nerve growth cone. *J. Neurobiol.* 44:114–125.

Kuhn, T. B., C. V. Williams, P. Dou, and S. B. Kater. 1998. Laminin directs growth cone navigation via two temporally and functionally distinct calcium signals. *J. Neurosci.* 18:184–194.

Letourneau, P. C., T. A. Shattuck, and A. H. Ressler. 1987. ''Pull'' ad ''push'' in neurite elongation: observations on the effects of different concentrations of cytochalasin B and taxol. *Cell Motil. Cytoskeleton.* 8:193–209.

Lin, C. H., and P. Forscher. 1995. Growth cone advance is inversely proportional to retrograde F-actin flow. *Neuron.* 14:763–771.

Marsh, L., and P. C. Letourneau. 1984. Growth of neurites without filopodial or lamellipodial activity in the presence of cytochalasin B. *J. Cell Biol.* 99:2041–2047.

Mitchison, T., and M. Kirschner. 1988. Cytoskeletal dynamics and nerve growth. *Neuron.* 1:761–772.

Novak, K. D., and M. A. Titus. 1997. Myosin I overexpression impairs cell migration. *J. Cell Biol.* 136:633–647.

O'Connor, T. P., J. S. Duerr, and D. Bentley. 1990. Pioneer growth cone steering decisions mediated by single filopodial contacts in situ. *J. Neurosci.* 10:3935–3946.

Othmer, H. G., S. R. Dunbar, and W. Alt. 1988. Models of dispersal in biological systems. *J. Math. Biol.* 26:263–298.

Pearson, E. S., and H. O. Harley. 1970. Biometrika Tables for Statisticians. Cambridge University Press, Cambridge.

Press, W. H., B. P. Flannery, S. A. Teukolsky, and W. T. Vetterling. 1986. Numerical Recipes: The Art of Scientific Computing. Cambridge University Press, Cambridge.

Soll, D. R., and E. Voss. 1998. Two- and three-dimensional computer systems for analyzing how cells crawl. *In* Motion Analysis of Living Cells. D. R. Soll, and D. Wessels, editors. Wiley-Liss, New York. 25–52.

Song, H. J., G. L. Ming, and M. M. Poo. 1997. cAMP-induced switching in turning direction of nerve growth cones. *Nature.* 388:275–279.

Stokes, C. L., and D. A. Lauffenburger. 1991. Migration of individual microvessel endothelial cells: stochastic model and parameter measurement. *J. Cell Sci.* 99:419–430.

Takei, K., R. M. Shin, T. Inoue, K. Kato, and K. Mikoshiba. 1998. Regulation of nerve growth mediated by inositol 1,4,5-trisphosphate receptors in growth cones. *Science.* 282:1705–1708.

Tessier-Lavigne, M., and C. S. Goodman. 1996. The molecular biology of axon guidance. *Science*. 274:1123–1133.

Uhlenbeck, G. E., and L. S. Ornstein. 1930. On the theory of the Brownian motion. *Phys. Rev.* 36:823–841.

Wagner, M. C., B. Barylko, and J. P. Albanesi. 1992. Tissue distribution and subcellular localization of mammalian myosin I. *J. Cell Biol.* 119:163–170.

Wang, F. S., J. S. Wolenski, R. E. Cheney, M. S. Mooseker, and D. G. Jay. 1996. Function of myosin-V in filopodial extension of neuronal growth cones. *Science.* 273:660–663.

Wessels, D., M. Titus, and D. R. Soll. 1996. A *Dictyostelium* myosin I plays a crucial role in regulating the frequency of pseudopods formed on the substratum. *Cell Motil. Cytoskeleton.* 33:64–79.

Wylie, S. R., P. J. Wu, H. Patel, and P. D. Chantler. 1998. A conventional myosin motor drives neurite outgrowth. *Proc. Natl. Acad. Sci. USA.* 95:12967–12972.

Zheng, J., R. E. Buxbaum, and S. R. Heidemann. 1994a. Measurements of growth cone adhesion to culture surfaces by micromanipulation. *J. Cell Biol.* 127:2049–2060.

Zheng, J. Q., M. Felder, J. A. Connor, and M. M. Poo. 1994b. Turning of nerve growth cones induced by neurotransmitters. *Nature.* 368:140–144.

Zheng, J. Q., J. J. Wan, and M. M. Poo. 1996. Essential role of filopodia in chemotropic turning of nerve growth cone induced by a glutamate gradient. *J. Neurosci.* 16:1140–1149.